Draft version June 10, 2022
Typeset using LaTeX **twocolumn** style in AASTeX631

arXiv:2107.07529v2 [astro-ph.EP] 8 Jun 2022

Hiding Planets Near and Far: The Parameter Space of Hidden Companions for Known Planetary Systems

Thea H. Faridani [1,2] Smadar Naoz [1,2] Lingfeng Wei (魏凌枫) [3] and Will M. Farr [4,5]

[1] *Department of Physics and Astronomy, University of California, Los Angeles, CA 90095, USA*
[2] *Mani L. Bhaumik Institute for Theoretical Physics, Department of Physics and Astronomy, UCLA, Los Angeles, CA 90095, USA*
[3] *Center for Astrophysics and Space Sciences, University of California, San Diego, La Jolla, CA 92093, USA*
[4] *Department of Physics and Astronomy, Stony Brook University, Stony Brook NY 11794, USA*
[5] *Center for Computational Astrophysics, Flatiron Institute, 162 Fifth Avenue, New York, NY 10010, USA*

ABSTRACT

Recent ground and space-based observations show that stars with multiple planets are common in the galaxy. Most of these observational methods are biased toward detecting large planets near to their host stars. Because of these observational biases, these systems can hide small, close-in planets or far-orbiting (big or small) companions. These planets can still exert dynamical influence on known planets and have such influence exerted upon them in turn. In certain configurations, this influence can destabilize the system; in others, the star's gravitational influence can instead further stabilize the system. For example, in systems with planets close to the host star, effects arising from general relativity can help to stabilize the configuration. We derive criteria for hidden planets orbiting both beyond and within known planets that quantify how strongly general relativistic effects can stabilize systems that would otherwise be unstable. As a proof-of-concept, we investigate the several planets in a system based on Kepler 56, and show that the outermost planet will not disrupt the system even at high eccentricities, and show that an Earth-radius planet could be stable within this system if it orbits below 0.08 au. Furthermore, we provide specific predictions to known observed systems by constraining the parameter space of possible hidden planets.

Keywords: Dynamical evolution (421), Exoplanet dynamics (490), General relativity (641), Planetary dynamics (2173), Star-planet interactions (2177)

1. INTRODUCTION

Recent developments in ground and space based observations have found that multi-planet systems are common in the Galaxy (e.g., Howard et al. 2010, 2012; Lissauer et al. 2011). Current leading exoplanet detection methods are are more sensitive to larger planets and to planets with shorter periods. For example, the popular transit method is particularly sensitive to close-in planets (Borucki 2016).

Because the transit method represents on the order of three quarters of all current exoplanet detections, the biases inherent in the method leave open two classes of planets that are currently difficult to detect: small planets close to their hosts and large planets further out. Radial velocity detection methods, as the second most prolific method, give access to large regimes of wide-orbit parameter space, and have shed light on the life cycle of giant planets living there (Hatzes et al. 2005; Knutson et al. 2014; Stock et al. 2018).

The observed statistical properties of multi-planet systems have been used to infer the underlying history and evolution of planets (e.g., Fang & Margot 2012; Hansen & Murray 2013; Malhotra 2015; Pu & Wu 2015; Steffen & Hwang 2015; Ballard & Johnson 2016; Xie et al. 2016; Weiss et al. 2018a; Pu & Lai 2018; Denham et al. 2019; Tamayo et al. 2020). One curious property of the multiplanet systems that have been observed is that the radii of planets in the same system are correlated with one another (Weiss et al. 2018a,b). There was debate whether this has been conclusively demonstrated to arise from formation processes as opposed to observation bi-

Corresponding author: Thea H. Faridani
thfaridani@astro.ucla.edu

ases (e.g., Zhu 2020; Weiss & Petigura 2020; Murchikova & Tremaine 2020), considering that dynamical evolution may erase the initial conditions of formation, however, correlations not explainable by observation bias have been demonstrated (e.g., He et al. 2021; Gilbert & Fabrycky 2020). Therefore, when we consider hypothetical configurations of planets that are meant to be similar to configurations already observed, we usually assume correlated planet masses.

Observations suggest that far-away companions (giant planets or even stars) are expected to host inner multi-planet systems. This trend was suggested by radial velocity surveys that showed a population of giant planets may exist at large distances from stars that host one or more inner planets (e.g., Knutson et al. 2014; Konopacky et al. 2016; Zhu & Wu 2018; Bryan et al. 2016, 2019). Additionally, several systems have been discovered where the configuration is strictly hierarchical, with a giant planet on a wide orbit outside of one or more very close-in planets (e.g., Bonomo et al. 2017; Ment et al. 2018; Barbato et al. 2018; Mills et al. 2019; Bryan et al. 2019; Zhu & Wu 2018). Furthermore, the most generic example is our solar system, with Jupiter at 5 au. Lastly, since the majority of stars exist in a binary configuration (e.g., Raghavan et al. 2010; Moe & Di Stefano 2015), a population of distant stellar companions to multi-planet systems is to be expected.

Companions that may exist far away from their host stars may dynamically affect an inner planetary system. For example, gravitational perturbations from a far-away companion (either a stellar or planetary companion) can excite the inner planets' eccentricity, via the Eccentric Kozai-Lidov (EKL) mechanism (e.g., Kozai 1962; Lidov 1962; Naoz 2016). High eccentricity, in combination with tidal dissipation, can lead to shrinking of the semi-major axis of a planet, circularizing it (e.g., Fabrycky et al. 2007; Wu et al. 2007; Naoz et al. 2011, 2012; Li et al. 2014a; Rice 2015; Petrovich 2015a; Lai et al. 2018; Stephan et al. 2018; Martin et al. 2015). On the other hand, the eccentricity excitations may plunge the planet into the star (e.g., Naoz et al. 2012; Petrovich 2015b; Lai et al. 2018; Stephan et al. 2018, 2020). In some cases, short-range forces, such as general relativity and tidal precession may suppress these eccentricity excitations (e.g., Fabrycky et al. 2007; Naoz et al. 2013a; Liu et al. 2015; Mardling & Lin 2004; Plavchan et al. 2015). In general, during the formation of planets, Jupiter-size planets have a large role in the final structure of the system, by driving planetesimals inward (e.g., Morbidelli & Crida 2007; Raymond & Izidoro 2017) or by controlling the ability of planetesimals to accrete (e.g., Hansen 2009; Walsh et al. 2011).

In the case of a multi-planet system, high eccentricity may result in destabilization. However, the gravitational interactions between close-by multi-planetary orbits, and in particular, the angular momentum exchange between different planets, may suppress high eccentricity induced by a far-away companion (e.g., Innanen et al. 1997; Li et al. 2014b; Hansen 2017; Pu & Lai 2018; Denham et al. 2019; Wei et al. 2021; Veras & Ford 2010; Holman & Wiegert 1999; Naoz et al. 2013b). Additionally, it may result in synchronized oscillation of the inclinations of all inner planets, resulting in a large obliquity—an observational marker that there may be a hidden far-away companion (e.g., Innanen et al. 1997; Takeda & Rasio 2005; Takeda et al. 2008; Li et al. 2014b; Denham et al. 2019; Boué & Fabrycky 2014).

On the other extreme, the lower mass limit of transit surveys today lies on the order of half an Earth radius, for a 1 $M_\odot$ host star (assuming a favorable noise level Christiansen et al. 2012). These short-period planets, usually said to have "ultra short periods" (USPs) of less than one day, produce so many transits that they can be detected despite their small size. Already, over a hundred such planets have been detected (e.g., Sanchis-Ojeda et al. 2014; Xiu-Min & Jiang-Hui 2020; Dai et al. 2017). One of the key observed qualities of USPs is that they may have radii $\lesssim R_\oplus$. Their small radii have been hypothesized to have been linked to the large irradiances they receive (e.g., Frustagli et al. 2020). Currently, the properties of the atmospheres of USPs (if they have any atmosphere at all) are relatively unknown (Malavolta et al. 2018). Because some models explaining the super earth radius gap rely on strong stellar flux incoming to the star (e.g., Owen & Wu 2016, 2017; Petigura 2020; Loyd et al. 2020)[1], USPs may be ideal candidates for constraining these models. Similarly, a range of formation scenarios exist that can explain how these planets came to have such short periods, such as secular chaos and disk migration (e.g., Pu & Lai 2019; Carrera et al. 2019; Petrovich et al. 2019; Becker et al. 2020). Though most models predict that they do not form completely *in situ*, at what stage in their evolution they are brought close to the star remains unclear (e.g., Millholland & Spalding 2020).

In this work, we examine the stability of planets in the radius and orbit ranges where their detection via the transit method is currently not possible. Historically, the techniques used in this work have exclusively predicted the permitted locations of large, distant com-

[1] We note that there are alternatives to the photo-evaporation model (see Gupta & Schlichting 2020, 2021).

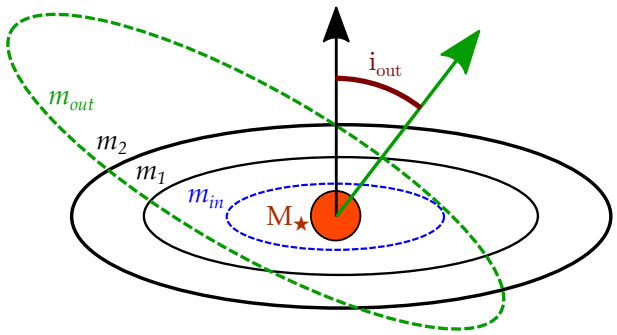


Figure 1. Schematic diagram (not to scale) of the systems discussed in this paper. A star of mass $M_\star$ has one or two known planets, m_1 and m_2. We will consider the stability of this system after the insertion of a hypothetical inner planet $m_{\rm in}$, or a hypothetical outer planet $m_{\rm out}$.

panion planets (e.g., Denham et al. 2019; Pu & Lai 2018). We extend these approaches by incorporating non-Newtonian forces arising from General Relativity (GR), allowing for constraints to be placed on short-period planets as well. In particular, we demonstrate, as a proof of concept, the usage of this analytical stability criterion for several hypothetical and observational examples.

This paper is structured as follows. In Section 2 we introduce the basic equations used throughout the analysis and show their use in quantifying the stability of systems. We then focus on systems with known two or more planets and put constraints on which of those systems have their stability against perturbation from an outer companion extended by GR precession (see Section 3). We then turn our attention to possible ultra-short period planets (USPs) (Section 4), and explore the role of GR for these systems (see for the derivation of an analytical stability criterion in Section 4.1). GR precession of USPs tends to suppress eccentricity excitations that may be induced due to Laplace-Lagrange resonances (as shown in Section 4.2. We then show that our USPs' stability analytical criterion agrees compared to numerical direct n-body integration (see Section 4.3).

In Section 5, as a case study, we examine the system Kepler 56 and explore the interaction between general relativity and traditional secular methods within it. Finally, in Section 6 we discuss our findings.

2. THE TWO KNOWN PLANETS - BASIC EQUATIONS

We consider a fiducial system composed of a star $M_\star$ with two observed planets, m_1 and m_2, and explore the possibility that a planet may be hiding undetected inward ($m_{\rm in}$) or outward ($m_{\rm out}$) of the known planets (see Figure 1 for an illustration of the system). The known planets have semi-major axes (eccentricities), denoted by a_1 and a_2 (e_1 and e_2) where $a_1 < a_2$. Angular momentum exchange between the inner planets may stabilize them against gravitational perturbations from the outer companion (e.g., Denham et al. 2019). Additionally, general relativity precession of the periapsis may instead further stabilize the system, including a possible inner planet from the perturbations of its neighbors.

Here we describe the basic equations that govern the system. The exchange of angular momentum between planets planets in the systems is described via the Laplace-Lagrange formalism. Given planets with masses m_j and m_k, the characteristic timescale over which the angular momentum of planet j changes due to planet k, can be written as:

$$\tau_{jk,\rm LL} = \left[A_{jj} + A_{jk}\left(\frac{e_k}{e_j}\right)\cos\left(\varpi_k - \varpi_j\right) - B_{jj} - B_{jk}\left(\frac{i_k}{i_j}\right)\cos\left(\Omega_k - \Omega_j\right)\right]^{-1} , \quad (1)$$

where e_j (e_k) is the eccentricity, and i_j (i_j) is the inclination of planet j (k) and Ω_j (Ω_k) is the longitude of ascending nodes of planet j (k), while ϖ_j (ϖ_k) is the longitude of periapsis. The coefficients A_{jk} and B_{jk} are given by (e.g., Murray & Dermott 2000):

$$A_{jj} = \frac{n_j m_k}{4\pi\left(M + m_j\right)}\alpha_{jk}\overline{\alpha}_{jk} f_\psi , \quad (2)$$

$$A_{jk} = -\frac{n_j m_k}{4\pi\left(M + m_j\right)}\alpha_{jk}\overline{\alpha}_{jk} f_{2\psi} , \quad (3)$$

$$B_{jj} = -\frac{n_j m_k}{4\pi\left(M + m_j\right)}\alpha_{jk}\overline{\alpha}_{jk} f_\psi , \quad (4)$$

$$B_{jk} = \frac{n_j m_k}{4\pi\left(M + m_j\right)}\alpha_{jk}\overline{\alpha}_{jk} f_\psi , \quad (5)$$

where,

$$\alpha_{jk} = \min\left(\frac{a_j}{a_k}, \frac{a_k}{a_j}\right) , \quad (6)$$

$$\overline{\alpha}_{jk} = \min\left(\frac{a_j}{a_k}, 1\right) , \quad (7)$$

and

$$f_\psi = \int_0^{2\pi} \frac{\cos\psi}{\left(\alpha_{jk}^2 - 2\alpha_{jk}\cos\psi + 1\right)^{3/2}} d\psi , \quad (8)$$

$$f_{2\psi} = \int_0^{2\pi} \frac{\cos 2\psi}{\left(\alpha_{jk}^2 - 2\alpha_{jk}\cos\psi + 1\right)^{3/2}} d\psi . \quad (9)$$

We assume that the two known planets were born *in situ*, i.e., their eccentricities and mutual inclinations are small and similar in value. We note that this not a universally advisable assumption. Under this assumption, the precession of the orbit of planet j due to the aforementioned angular momentum exchange with planet k takes place over a characteristic timescale, estimated as:

$$\tau_{LL,jk} = \left[\frac{n_j m_k}{4\pi(M_\star + m_k)}\alpha_{jk}\overline{\alpha}_{jk}\left(f_\psi \pm f_{2\psi}\right)\right]^{-1} , \quad (10)$$

where n_j is the mean motion of planet j, and the two cases $(f_\psi \pm f_{2\psi})$ correspond to the the minimum $(+)$ and maximum $(-)$ values this timescale can achieve.

Neither f_ψ nor $f_{2\psi}$ have a known closed-form representation to our knowledge, but under the assumption that $\alpha_{jk} \leq 0.9$, we find

$$(f_\psi - f_{2\psi}) \approx 7\alpha_{jk} , \quad (11)$$

to within an error of not more than 40%. Because this term has a simple closed-form approximation, when deriving our criterion, we use the $(f_\psi - f_{2\psi})$ case over the $(f_\psi + f_{2\psi})$

In addition to the Newtonian effect between the two planets, general relativity produces a precession of their orbits. Thus, a far away companion may drive high eccentricity on the inner planets, but in addition to stabilization from Laplace-Lagrange interaction, general relativity precession may suppress this eccentricity excitation (Wei et al. 2021). The timescale of apsidal precession on planet j caused by general relativity is given by (e.g., Naoz et al. 2013b)

$$\tau_{GR,j} = 2\pi\frac{c^2 a_j^{5/2}(1-e_j^2)}{3(GM_\star)^{3/2}} , \quad (12)$$

where c is the speed of light.

3. AN OUTER COMPANION: THE ROLE OF GR FOR KNOWN SYSTEMS

Consider an outer, inclined companion ($m_{\rm out}$) to two inner planets (m_1, m_2) that satisfy $a_1 < a_2$. Including this outer companion makes the system hierarchical. This outer companion may excite the eccentricities of the inner planets through the EKL mechanism (e.g., Naoz 2016). The associated timescale for this eccentricity excitation on an inner planet j is given by (e.g., Antognini 2015)

$$\tau_{\rm EKL,j} = \frac{16}{15}\frac{a_{\rm out}^3\left(1-e_{\rm out}^2\right)^{3/2}\sqrt{\left(M_\star + m_j\right)/G}}{a_j^{3/2} m_{\rm out}} , \quad (13)$$

where $a_{\rm out}$ is the outer companion semi-major axis. On the other hand, Laplace-Lagrange interactions, which exchange angular momentum between the inner planets, can suppress the outer companion's induced eccentricity excitations (e.g., Innanen et al. 1997; Takeda & Rasio 2005; Takeda et al. 2008; Li et al. 2014b; Pu & Lai 2018; Denham et al. 2019). For the suppression to occur, the angular momentum exchange due to Laplace-Lagrange interactions, needs to take place on a shorter timescale than the EKL typical timescale. The timescale of the Laplace-Lagrange effect on planet 2's orbit from the gravity of planet 1 is approximately (see Equation (1)):

$$\tau_{\rm LL,21,max} \approx \left[\frac{7 n_2 m_1}{4\pi M_\star}\left(\frac{a_1}{a_2}\right)^2\right]^{-1} . \quad (14)$$

Denham et al. (2019) derive an analytical stability criterion indicating the region of parameter space in which a two-planet system is stable against gravitational perturbations from a far away companion. However, short range forces can also tend to stabilize a system (this was noted in the three body systems, e.g., Ford et al. 2000; Naoz et al. 2013b; Liu et al. 2015; Hansen & Naoz 2020). Recently Wei et al. (2021) generalized the aforementioned stability criterion to include general short range forces. In particular, here we consider general relativity precession due to the star[2].

As was shown in Wei et al. (2021) general relativity can only extend the stability regime beyond what was shown by Denham et al. (2019) if the GR timescale is shorter than the Laplace-Lagrange timescale between the two inner planets. In other words, if the timescale hierarchy is such that $\tau_{\rm GR,2} < \tau_{\rm EKL,2}$, but $\tau_{\rm GR,2} > \tau_{\rm LL,21}$ then the system will be stable against EKL excitation by the outer perturber (as shown by Denham et al. 2019), but may still be susceptible to detail-dependent excitations by Laplace-Lagrange, as we will discuss in section 4.

Considering the population of known two-body systems, we ask in which systems GR effects further help stabilize the system more than the stabilization achieved by Laplace-Lagrange. Observed two-body systems are likely to be stable (or marginally stable) because they have survived long enough for us to observe them. In such a system, if there is an outer perturber, the outermost known planet is affected by the perturber's EKL excitations more than the inner known planet. Thus, if a hidden companion exists, and GR is assumed not to

[2] Tidal precession is also a relevant short-range force that may work to stabilize the system. General relativity precession is often more important compared to tidal precession (e.g., Fabrycky & Tremaine 2007; Liu et al. 2015).

be relevant, the timescale hierarchy is $\tau_{\rm EKL,2} > \tau_{\rm LL,21}$. Therefore, to examine the importance of GR effects, we must ask when does GR stabilize m_2 against EKL more than Laplace-Lagrange does, i.e., when EKL excitation is involved, GR is necessary to include only when $\tau_{\rm GR,2} < \tau_{\rm LL,21,max}$, which produces the criterion:

$$\frac{a_1^2}{a_2} \leq \frac{6GM_\star^2}{7c^2(1-e_{\rm max}^2)m_1}, \tag{15}$$

where we used the approximation in Equation (11). Using $\tau_{\rm LL,21,min}$, we do not have a neat approximation for $(f_\psi + f_{2\psi})$, so the criterion becomes

$$a_1\,(f_\psi + f_{2\psi}) \leq \frac{6GM_\star^2}{c^2(1-e_{\rm max}^2)m_1}. \tag{16}$$

In these equations, $e_{\rm max}$ represents the maximum eccentricity induced by the quadrupole-level, EKL oscillation in the presence of general relativity. Aside from $e_{\rm max}$, none of the terms in these criteria depend on the parameters of the outer perturber inducing the EKL oscillation. In other words, to evaluate whether GR is important when considering EKL oscillation from an outer companion, we only need to consider the eccentricity it induces on m_2. This is shown in Figure 2, where we depict a population of 2-planet systems, with the diagonal lines indicating different choices of $e_{\rm max}$. Thus, potentially highlighting that for a small but not insignificant fraction of 2-planet population (4-5%), GR plays an important role in stabilizing the system.

Figure 2 depicts known two-planet systems, adopted from the `exoplanet archive` (NASA Exoplanet Archive 2022), in the parameter space defined by the plane a_1^2/a_2-M^2/m, motivated by Equation (15). We have removed systems orbiting binary stars, systems without measurements of stellar mass or where one or both of the two planets lack mass measurements. Overplotted are the boundary lines between GR dominating and Laplace-Lagrange dominating as a function of $e_{\rm max}$. To first-order, e_{max} represents the maximum eccentricity that would be obtained within a few EKL or Laplace-Lagrange cycles in the presence of GR precession, which is straightforward to calculate (e.g., Fabrycky & Tremaine 2007; Liu et al. 2015). The value of e_{max}, can be extremely high, even in the presence of GR precession (e.g., Naoz et al. 2013b; Teyssandier et al. 2013; Li et al. 2014a). We note that at values of $e_{max} > 0.8$ much of the parameter space lies below the transition curve, meaning that if $e_{\rm max}$ is high, GR is making a significant contribution to the stability of a non-negligible portion of the parameter space. It is worthwhile to point out that the Laplace-Lagrange formalism is an expansion in small eccentricities. However,

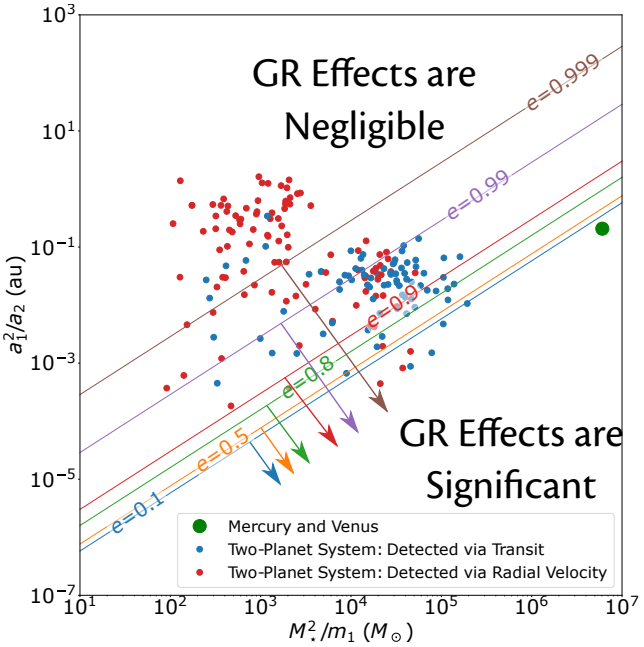


Figure 2. Susceptibility of known, two-planet systems to GR necessity. Systems without measured stellar masses are not included. Known two-planet systems (blue and red for planets detected by the Transit Method and the Radial Velocity method, respectively) in the parameter space defined by Equation (15), which defines the a_1^2/a_2 - M^2/m plane. Overplotted are lines for different $e_{\rm max}$ that can be induced by EKL. Below the lines $\tau_{\rm GR}(m_2) < \tau_{\rm LL}$. Plotted in green is the Mercury-Venus pair. Systems lying below a given curve have their stability against EKL excitation extended by GR. Notably, At moderate-to-large values $e_{\rm max}$, the inclusion of GR extends the stability regime of a significant number of systems.

even when higher orders in eccentricity are included, the combination of the GR and Laplace-Lagrange precessions can accurately predicate the stability criterion, as shown in Wei et al. (2021). Note that other processes, especially when high mutual inclinations, and high eccentricities may exist, and higher orders of the approximation can affect the system (e.g., Naoz 2016).

4. AN INNER COMPANION

Most exoplanet detection methods are sensitive to short orbital periods. For example, the Kepler telescope's data pipeline could detect planets on a 1.5 year orbit at the longest (because of the pipeline's requirement of 3 or more transits). Furthermore, Kepler's methods are insensitive to planets with radii smaller than about $0.5\,R_\oplus$. For Earth-mass planets it is also insensitive to whose with orbital periods longer than

about 150 days (see Fig 1 of Christiansen 2017).[3] Thus, if two planets were detected in a system, an inner planet may still be hidden there with a radius smaller than $R_\oplus$. We now investigate the stability of such a planet under perturbations from its companions.

4.1. *The Role of GR - Stability Criterion for Inner Companion*

We now consider systems where a small (Super-Earth or lighter) planet ($m_{\rm in}$) orbits within one or more other planets with small mutual inclinations and arbitrary masses (see Figure 1). In this scenario, without an outer companion, the EKL mechanism is not pronounced, and the system is non-hierarchical, but significant eccentricities up to ~ 0.4 can still be driven on the super-earth by Laplace-Lagrange effects (see also Section 4.2 for example).

Depending on the orbital configuration, this could fatally disrupt this planet. However, if GR precession occurs on a shorter timescale than Laplace-Lagrange excitation, then the eccentricity that can be excited drops significantly. Because we are now concerned with the stability of the innermost planet, we must use the GR precession timescale of the inner planet, $\tau_{\rm GR,in}$ and require stability against Laplace Lagrange excitations from the further-orbiting m_1 on m_{in}. Note that in Section 3, we consider the Laplace-Lagrange interactions between m_1 and m_2, where the latter is influenced by a distant companion (with an arbitrary geometry). Here we consider a different structure, where m_1 and m_2 are perturbing a hidden planet $m_{\rm in}$ (See Figure 1 for an illustration of the system). We wish again to compare the Laplace-Lagrange and GR timescales as we did in Eq (15) to investigate stability. However, the new structure changes the semi-major axis dependence of the Laplace-Lagrange timescale (see Eq (10) for details), so a new criterion must be derived. The Laplace-Lagrange timescale acting on m_{in} from the perturbations of m_1 is given by Eq. (10):

$$\tau_{\rm LL,in1,max} \approx \left[\frac{7 n_{in} m_1}{4\pi M_\star}\left(\frac{a_{in}}{a_1}\right)^3\right]^{-1} , \qquad (17)$$

$$\tau_{\rm LL,in1,min} = \left[\frac{n_{in} m_1}{4\pi M_\star}\left(\frac{a_{in}}{a_1}\right)^2 (f_\psi + f_{2\psi})\right]^{-1} . \qquad (18)$$

[3] Stellar and especially stellar activity may push this limit up and down. For example, the $0.354\,R_\oplus$ planet Kepler 37b was discovered in 2013 orbiting an especially quiet star (e.g., Barclay et al. 2013).

Thus, the stability criterion of $\tau_{\rm GR,in} < \tau_{\rm LL,in1}$ yields (using $\tau_{\rm LL,in1,max}$):

$$\frac{a_{\rm in}^4}{a_1^3} \leq \frac{6GM_\star^2}{7c^2(1-e_{\rm max}^2)m_1} , \qquad (19)$$

and using $\tau_{\rm LL,in1,min}$)

$$\frac{a_{\rm in}^3}{a_1^2}(f_\psi + f_{2\psi}) \leq \frac{6GM_\star^2}{c^2(1-e_{\rm max}^2)m_1} , \qquad (20)$$

where $e_{\rm max}$, is the maximum eccentricity achieved by $m_{\rm in}$ due to Laplace Lagrange resonance.

4.2. *Example of Resonances in Laplace-Lagrange Secular Evolution*

The Laplace-Lagrange secular model has an analytical solution, where the eccentricity and inclination are, as functions of time, algebraic functions of sines/cosines of eigenfrequencies (Murray & Dermott 2000, p.277-278). Therefore, there exist some configurations of planets where these eigenfrequencies approach one another in value, driving large eccentricities and inclinations in what we call a "Laplace-Lagrange Resonance". Because the Laplace-Lagrange model assumes eccentricities remain low, and at these resonance points it can predict extreme eccentricity values, the assumptions implicit in Laplace-Lagrange formalism may be violated in these configurations. Thus, n-body simulations may result in higher but not necessarily unity eccentricities. Given two fixed planets, the semi-major axis values where a third planet would be in resonance are not affected by the masses of the two fixed planets. The relative masses of the planets do, however, affect the eccentricity the resonance predicts: if a planet is in resonance and is significantly less massive than its companions, its eccentricity will be excited to larger values.

Angular momentum exchange between planetary orbits via the Laplace-Lagrange perturbations can result in eccentricity excitations even in the absence of an outer companion. In Figure 3, bottom panel, we show the maximum eccentricity reached for an Earth-mass planet set at different separations as predicted from Laplace-Lagrange equations. As a case study we consider the HD 15337 system, which is composed of $M_\star = 0.9\,M_\odot$ and has two planets with the following parameters: $a_1 = 0.0522$ au, $m_1 = 7.51\,M_\oplus$, and $a_2 = 0.1268$ au, $m_2 = 8.11\,M_\oplus$ (Gandolfi et al. 2019). In the bottom panel of Figure 3, we show the maximum eccentricity predicted by Laplace-Lagrange's aforementioned analytical solution, as a function of a hypothetical inner planet's semi-major axis. This calculation is done in the $m_{\rm in} \to 0$ test-particle limit. Outside of this approximation, if $m_{\rm in}$ is set close to m_1 and m_2, the height of

the resonance peaks decrease, but their locations as a function of $a_{\rm in}$ do not change.

We consider a test case of two specific points, one on-resonance, and one off-resonance. Here "on-resonance" refers to a configuration where multiple frequencies in the A matrix (2) are close or equal in value, resulting in large predicted eccentricities for one (or more) of the planets in the system. For both of them we use the n-body code `MERCURY`, integrating over 5×10^5 yrs (Chambers 1999). This version of `MERCURY`, accounts for general relativity precession from the 1st post-Newtonian term, (M. Payne private communication). Here the Earth-mass planet eccentricity is initially set with $e = 0.1$, and negligible mutual inclination with the known planets in the system. As depicted (top left panel in Figure 3), over most of the parameter space, the eccentricity is excited up to about 0.2–0.3, with fluctuation around that eccentricity possible in a configuration of Laplace-Lagrange resonance. On the other hand, (top right panel in Figure 3), when the GR precession timescale is shorter than the typical Laplace-Lagrange precession, these eccentricity excitations is suppressed. In general, we find that regardless of whether this system is set up in a resonant configuration or not, when general relativity precession is included in the simulations, its timescale is short enough (by a factor of about 200 in the resonant configuration) to dominate over Laplace-Lagrange and force the eccentricity to remain at its initial value. We also note that general relativity precession is indeed damping out the Laplace-Lagrange resonance rather than simply shifting the eccentricity peak to another location.

On the margins of the Laplace-Lagrange timescale/GR timescale equality, whether a resonance can destabilize a system where the GR timescale and the Laplace-Lagrange timescale differ by only a factor of unity is detail-dependent[4]. However, we find that when the GR timescale is hundreds to thousands times shorter than the Laplace-Lagrange timescale, even resonances tend to be damped out.

4.3. *Numerical Comparison*

Next we test our stability criterion, Equation (19) for the inclusion of a hidden inner planet against secular simulations. We utilize the Gauss averaging method to integrate the system, while including 1st Post Newtonian GR precession (c.f. Wei et al. 2021). In this approximation the line density of an orbit is inversely proportional to the velocity (e.g., Touma et al. 2009). This type of analysis was shown to be very efficient in calculating long-term evolution (e.g., Nesvold et al. 2016; Denham et al. 2019; Wei et al. 2021; Michtchenko & Malhotra 2004). The secular code allows us to study the system for long timescales as we note that the secular code agrees with the n-body code `MERCURY`, (Chambers 1999) with general relativity (M. Payne private communication).

As a case study, we consider the HD 106315 system (Zhou et al. 2018; Livingston et al. 2018), which consist of a 1.024 $M_\odot$ star and two known planets: HD 106315 b (c) with mass 12.6 $M_\oplus$ (15.2 $M_\oplus$), semi-major axis 0.097 au (0.154 au), and eccentricity 0.093 (0.22) (e.g, Barros et al. 2017; Mayo et al. 2018; Crossfield et al. 2017; Rodriguez et al. 2017). We consider a possible hypothetical

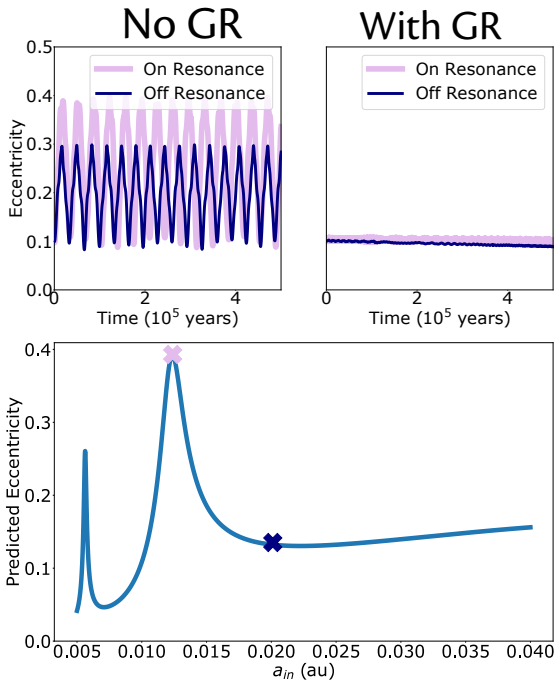


Figure 3. An Earth-mass planet was inserted within HD 15337's two orbits at a semi-major axis of peak resonance, 0.0125 au (marked in light pink), and once off-resonance at 0.02 au (marked in dark blue) both with an initial eccentricity of $e_{\rm in} = 0.01$ and integrated forward 50,000 years using the n-body code `MERCURY`. HD 15337 is a 0.9 $M_\odot$ star that hosts two known planets with $a_1 = 0.0522$ au, $m_1 = 7.51\,M_\oplus$, and $a_2 = 0.1268$ au, $m_2 = 8.11\,M_\oplus$ (Gandolfi et al. 2019). In the top panels the eccentricities both with (right) and without (left) including GR are plotted. In the bottom panel we show the maximum eccentricity the Laplace Lagrange formalism predicts the planet should achieve over long timescales. The behavior of the eccentricity of the test planet is strongly effected by the predicted resonance, and in the presence of GR, the resonance is completely damped out.

[4] Similarly to the resonant-like behaviour that takes place when GR precession on a similar timescale to that of a quadrupole-level hierarchical three body system (e.g. Naoz et al. 2013b).

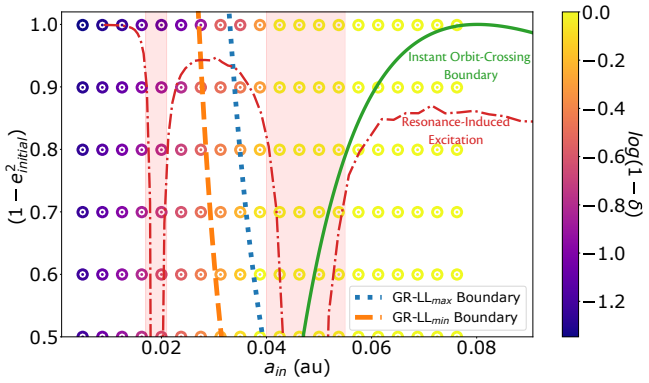


Figure 4. Stability map of a hypothetical-inner planet. In particular, we consider the HD 106315, composed out of two planets, HD 106315 b (c) with mass $12.6\,M_\oplus$ ($15.2\,M_\oplus$), semi-major axis 0.097 au (0.154 au). We show the inner planet's initial specific angular momentum, as $1-e^2_{\rm initial}$ as a function of it's semi-major axis $a_{\rm in}$ (here, $e_{initial}$ spans the range from 0.01 at the top, to 0.71 at the bottom). The mass of the inner planet is $0.1\,M_\oplus$. The points show the numerical integration of the system up to 1 Myr, where the color code represents how close the two orbits came to crossing over the integration according to Eq. (21). The dot-dashed red line shows the Laplace-Lagrange prediction of the hidden planet's eccentricity, and regions where this eccentricity is especially high–the resonances–are shaded red. We over plot the GR-Laplace-Lagrange boundary according to Eqs. (19) and (20), thick, dashed orange, and dotted blue, respectively. We expect that to the left of these boundaries systems GR precession will suppress eccentricity excitations due to Laplace-Lagrange resonances, and to the right of these boundaries, resonances may lead to orbit crossing. Finally, the green line shows the orbit crossing limit.

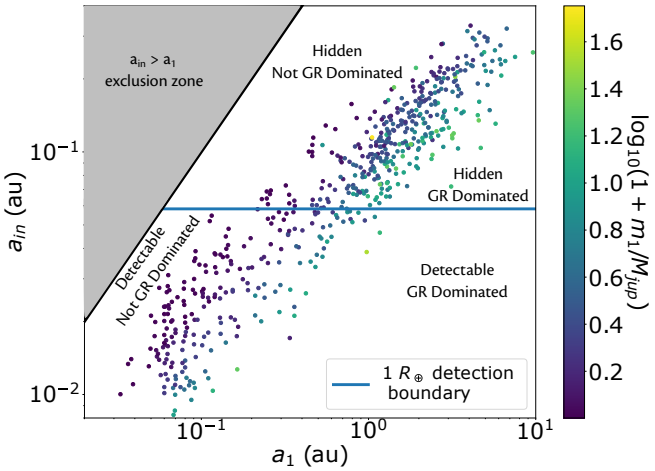


Figure 5. The relationship between the semi-major axis of the shortest observed orbit in a system (a_1) and the largest possible semi-major axis a hypothetical inner planet could have while still being GR dominated (see Eq. (19)). Each dot represents a known main sequence star with either two or one known planets. The color represents the mass of the known planet m_1 in log. Overplotted is the boundary that separates the region where a $1\,R_\oplus$ inner planet would be detectable, via transit, according to Eq. (22) if orbiting a sunlike star. Closer orbits (smaller $a_{\rm in}$) are more likely to be detected via transits and RVs. The region of parameter space where $a_{in} > a_1$ has been grayed out as it is excluded by assumption. The inner planets were assumed to share Earth's mass and radius.

inner planet with $m_{\rm in} = 0.1 M_\oplus$ and explore the stable configuration of the system.

In Figure 4, we depict the hidden inner most planet's initial specific angular momentum ($1-e^2_{\rm initial}$), as a function of its semi-major axis $a_{\rm in}$). Following Denham et al. (2019), we quantify how close the orbits grow over the course of the simulation as:

$$\delta = \frac{a_1(1-e_1) - a_{\rm in}(1+e_{in,max})}{a_1 - a_{\rm in}}\,, \qquad (21)$$

shown through the coloring of the dots. We highlight the locations of the Laplace-Lagrange resonances (the shaded regions), and the Laplace-Lagrange predicted eccentricity at all a_{in} values (the dot-dashed red line). We overplot our stability criterion, from Equation (19) as the dotted thick line as well as a modified version of the criterion where we use the minimum Laplace-Lagrange timescale instead of the maximum (dashed line, see Eq. (20)). To the right of the this boundary where Laplace-Lagrange dominates, we see that the secular resonance on the inner planet is enough to drive orbit crossing ($\delta \to 0$), but on the left side of the boundary, where GR dominates, the secular resonance does not induce any additional eccentricity—even when initial eccentricities are set to be as high as $1-e^2_{init} = 0.5$. We also see that the difference between using the minimum Laplace-Lagrange timescale instead of the maximum as we do in Equation (19) does not make a significant difference in the location of the boundary between Laplace-Lagrange and GR dominance.

To the right of the large resonance we can see in the low initial eccentricity runs that although they are beyond the resonant region, enough eccentricity is excited to achieve orbit crossing. This arises from the structure of the resonances. In systems with exactly two planets, where there are two resonances within the orbit of the closest-in planet, typically the region between the second resonance and a_1, has a maximum eccentricity higher than the region inward to the first resonance (as also shown in Figure 4, dot-dashed line, note that this effect is less pronounced in Figure 3, but still present). This behavior can drive orbital crossing even outside the resonant region.

4.4. *Observational Implications*

Figure 5 depicts the largest possible semi-major axis (a_{in}) that a hypothetical, earth-analogue inner planet could have while still remaining GR-dominated for an observed system. We show this as a function of the semi-major axis of the closest-in observed planet in the system (a_1). We limit the sample to planets orbiting main-sequence stars with two or fewer known planets. The points' colors represent the mass of the known planet, m_1. Below the points represents regions of parameter space where an inner planet would be GR dominated, above—Laplace-Lagrange dominated. For each star, a boundary exists where transiting planet can be detected (see Eq. (22)).

We use a simplified model of the Kepler mission pipeline's candidate confirmation requirement that the Multiple Event Statistic (MES) must be greater than 7.1 (Christiansen et al. 2012). The MES is given approximately by

$$\mathrm{MES} \approx \left(\frac{R_p}{R_\star}\right)^2 \frac{1}{CDPP_{eff}} \sqrt{N_t} \ , \tag{22}$$

where $R_\star$ (R_p) is the stellar (planet) radius, $CDPP_{eff}$ is the effective stellar noise in parts per million, and N_t is the number of transits the planet makes over the observing period. While this boundary depends on the stellar radius, as a proof-of-concept, here we over plot the semi-major axis a_{in} beyond which an earth-radius planet would be undetected, for a 1 $R_\odot$[5].

The dispersion around the trend reveals that among the set of main sequence stars around which planets have been found, the widest orbit an inner planet can have and remain GR dominated is determined by a_1 to within about an order of magnitude. Importantly, *in this case,* we need only information about one known planet in order to mark the locations in parameter space where a currently undetected planet may be hidden as is done in Figure 5. Therefore, by needing very little information as depicted in Figure 5, the number of systems to which this criterion is applicable is maximized.

For a particular system, the area above the detection boundary and below that system's associated point, marks the region of parameter space that is both hidden from current observation and is GR dominated. As we show in Figure 4, the GR dominated regime stabilizes such planets against Laplace-Lagrange eccentricity excitation. This Hidden and GR Dominated region of parameter space is more stable than non-GR dominated regions and more likely to contain planets than unstable regions. Notably, higher values of the known planets mass m_1 increases the strength of Laplace-Lagrange interactions between it and the inner planet. Thus, the largest allowable $a_{\rm in}$ where the inner planet is GR dominated must shrink as m_1 increases.

Notably, higher values of the known planet's mas m_1 make the largest GR dominated a_{in} in their systems smaller, thus shrinking the Hidden+GR Dominated portion of parameter space. Among systems where m_1 is less than a Jupiter mass, this region is quite a bit larger.

5. KEPLER-56: PROOF OF CONCEPT (OUTER AND INNER COMPANIONS)

Kepler-56 is a $1.32\,M_\odot$ red giant branch star, hosting three known planets (e.g. Huber et al. 2013; Otor et al. 2016; Lissauer et al. 2011; Hadden & Lithwick 2014). These planets feature a significant hierarchical structure—the semi-major axes of the three planets are 0.103, 0.165 and 2.16 au, with masses of $0.07\,M_J$ and $0.57\,M_J$ for the inner planets, respectively. The inner two planets exhibit large obliquity with respect to the star's spin axis (Huber et al. 2013). The outer planet is non-transiting, with an $M \sin i$ value of $5.61\,M_J$ (e.g. Otor et al. 2016). The two inner planets have small eccentricities (< 0.05), indicating that EKL excitations from Kepler-56d are not destabilizing this system, but can result in the large spin-orbit misalignment (Li et al. 2014b). The outer planet has eccentricity of ~ 0.2 (Otor et al. 2016). Indeed, applying the criterion defined in Denham et al. (2019), we find that the critical eccentricity of Kepler-56 d above which we expect large eccentricity fluctuation of these planets is ~ 0.83, much larger than its reported eccentricity.

Using Eq. (19), we can constrain a hypothetical Earth-radius planet in Kepler-56 to lie at less than $\lesssim 0.07$ au, depending on this planet's initial eccentricity. However, we find that a Mercury-radius planet with sufficient eccentricity can remain GR dominated at orbits wider than 0.08 au[6] but probably cannot be wider than 0.088 au, which represents about 5 mutual Hill radii from Kepler-56 b (the spacing that can yield stability against planet-planet scattering Chatterjee et al. 2008). From Eq. (22) we see that, such a planet could transit and remain undetected at orbits comparable to its Roche limit with the host star.

Because Kepler-56 contains a known outer planet, we observe the behavior of the system after the insertion of a hypothetical inner planet in Figure 6. We simulate the system both with and without GR in four configu-

[5] Note that the stellar radii of the observed systems in Figure 5, have a typical radius of 1 $R_\odot$, up to about a factor of 2.

[6] We note that the stability limits uses Eq. (11), which is valid when $a_1/a_2 < 0.9$, which somewhat limits the extent of the use of the equation.

rations depicted in the middle column of Figure 6. The first configuration has no inner planet, and the known outer planet has been removed. The second brings back the outer planet, and its eccentricity has been increased to $e_{\rm out} = 0.8$ to exaggerate its effect for proof of concept purposes. The third and fourth configurations introduce a hypothetical inner companion first at an orbit close to its neighboring planets where the GR and Laplace-Lagrange timescales are roughly equal, and second at an orbit close to the host star where the GR timescale dominates. For each configuration we plot the inclination of all the planets and their "orbital range" or the location of each planet's periapsis and apoapsis as functions of time. If one planets periapsis overlaps with another's apoapsis, we conclude the system will undergo an eventual orbit crossing and is likely unstable. The EKL timescale is smaller than both in all configurations, but because of Laplace-Lagrange and GR having weak influence over inclinations, the outer planet still causes large, synchronized inclination shifts. Broadly, we find that this system is quite stable even with the outer planet's eccentricity artificially increased. However, we find that in the third configuration, the hypothetical planet does undergo orbit crossing after 500,000 years, but only if GR is neglected. Because the outer known planet's eccentricity has been measured to be about $e_{\rm out} = 0.2$ (Otor et al. 2016), the system is even more stable than these plots show. This modified system is a valuable test case to show how a multiplanet system can be stable in the presence of an extreme companion (where we have adopted a higher eccentricity for the outer planet to more clearly demonstrate its effect) and a possible inner planet. We further demonstrate in Figure 6 third row that GR precession extends the stability regime.

6. DISCUSSION

Our current exoplanet detection methods are less effective at detecting smaller planets and far-orbiting planets than larger or closer-in planets. Already, for example, it is estimated that about 50% of stars may host Jupiter-like planets at wide separations (Bryan et al. 2016, $5 - 20$ au). In general it was suggested that a population of giant planets often host one or more inner planets (e.g., Knutson et al. 2014; Konopacky et al. 2016; Zhu & Wu 2018; Bryan et al. 2016, 2019). Further, some close-in small planets have already been observed (e.g., Sanchis-Ojeda et al. 2014; Xiu-Min & Jiang-Hui 2020; Dai et al. 2017). Here we study the stability of known, at most two-planet systems, hosting either a far away companion or a inward small planet.

We have quantified a condition under which the addition of a new planet into a known system does not destabilize the system, considering both inner and outer hypothetical planets. A far away companion, may excite the inner system's eccentricities, via the EKL mechanism driving them to instability. However, Laplace-Lagrange interactions between neighboring planets can tend to stabilize the system (Pu & Lai 2018; Denham et al. 2019). Recently Wei et al. (2021) showed that GR precession expands the stability regime. Here we consider all systems with more than one observed planet, and constrain the regimes where GR precession expands the stability of the system against EKL excitation more than Laplace-Lagrange on its own (depicted in Figure 2). This regime depends on the maximum eccentricity excited via EKL form the far-away companion which often can be extremely high (e.g., Li et al. 2014a).

Further, we developed analytic criteria for the stability of an inner planet (see Equations (19) and (20)). In this case, motivated by `Kepler` sample of "peas in the pod" (Weiss et al. 2018a), we assume a low-inclination planet inwards of a known planetary system. Laplace-Lagrange resonances can drive this inner planet to high eccentricity values. General relativity precession can suppress these eccentricity excitations, as highlighted in Figure 3. In some cases, Laplace-Lagrange resonances may drive the system to instability, i.e. orbital crossing. We show that our analytical criteria (Equations (19) and (20)) are in good agreement with numerical calculation, as depicted in Figure 4.

Using our analytical criterion we examined all systems with either one or two planets and estimated the largest possible, stable semi-major axis of a hypothetical planet (see Figure 5). A planet could be hidden in a system that is only Laplace-Lagrange dominated, but if a resonance exists, some locations my be unstable. On the other hand, the GR precession dominated regime will suppress Laplace-Lagrange resonances, making it a stable location for short period planets to exist (right side in Figure 5).

We note that stellar oblateness (also known as J2) can induce nodes precession of an ultra short planet. It was suggested that this precession may even result in inducing small mutual inclination between multi-planet systems ($\lesssim 40^\circ$ e.g., Becker et al. 2020; Li et al. 2020; Schultz et al. 2021). As highlighted in Wei et al. (2021), stability analysis can be done for wide variety of short-range forces. Thus, it is straightforward to estimate the induced precession due to the stellar rotation. We find that for a Sun-like star system, assuming a Sun-like rotation rate ($\sim$ 25 d period), the oblateness-induced precession timescale is much longer over most part of the parameter space (e.g., in Figures 4 and 5). However, we note that G-type stars probably slow their spin during

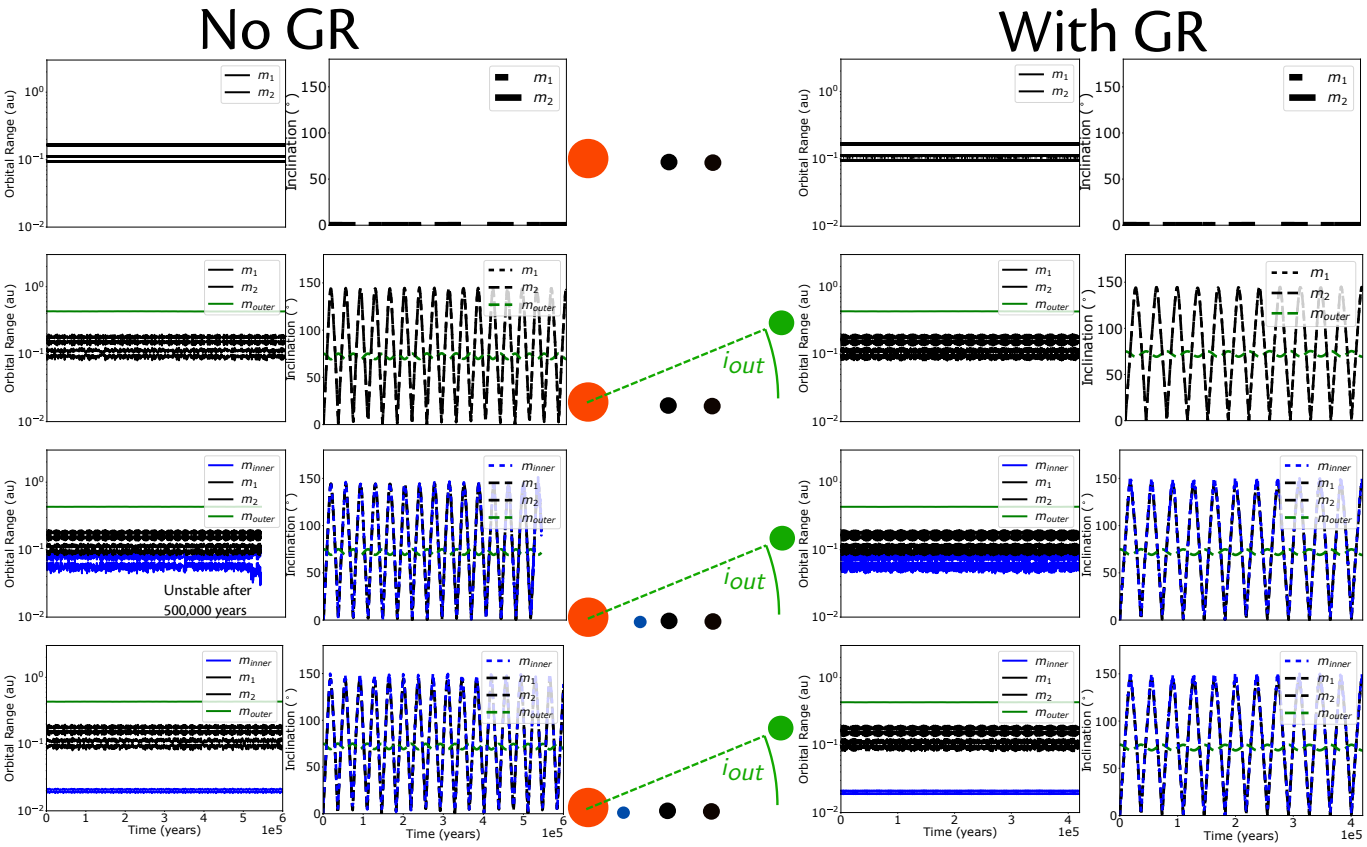


Figure 6. Orbital outcomes of our Kepler 56-like system in 4 configurations, with all 4 configurations run once without GR and once with GR. Top to bottom (as indicated by the cartoons in the middle) are the eccentricities and inclinations of the constituent planets when (i) The outermost planet is removed (ii) The outermost planet is included (iii) An Earth-mass planet is inserted into the system close to the innermost planet (iv) An Earth-mass planet is inserted into the system close to the star. Kepler 56 is a $1.32\,M_\odot$ star that hosts three known planets with $a_1 = 0.1028\,\mathrm{au}$, $m_1 = 0.58\,M_J$, $e_1 = 0.04$, $a_2 = 0.165\,\mathrm{au}$, $m_2 = 0.57\,M_J$, $e_2 = 0.01$, and $a_3 = 2.16\,\mathrm{au}$, $m_3 = 5.61\,M_J$ (Huber et al. 2013; Otor et al. 2016). We set $e_3 = 0.8$ rather than its measured value of about 0.2 for the purposes of proof-of-concept. The outer planet's inclination was set to $i_{\mathrm{out}} = 75°$. The inner planet is one Earth-mass and starts the integrations with negligible eccentricity

their evolution due to magnetic braking (e.g., Dobbs-Dixon et al. 2004). Thus, it may be that the oblateness-induced precession was more significant compared to GR precession, for young, fast spinning, stars.

Finally, we highlight the relevance of GR precession by considering the system, Kepler-56 (Huber et al. 2013), and starting with two-planet systems, we systematically add planets (see Figure 6 while comparing to evolution with and without GR. We first (second panel) add Kepler-56d, although for a proof-of-concept we adopt a higher eccentricity for it, 0.8. The system indeed is stable to even such high eccentric companion (e.g., Denham et al. 2019). We then add a smaller planet inward to Kepler-56b[7], and show two examples. One of which GR precession suppress eccentricity excitations, due to a resonant location, and another one, off-resonance. As shown in Figure 6, a combination of the Laplace-Lagrange and GR precessions stabilize an extreme Kepler-56 like system. In particular, an even more eccentric outer companion than the one observed can still keep the system stable (consistent with Denham et al. 2019). Moreover, the system can hide a hypothetical small companion, inward to Kepler 56b, and remain stable.

The aforementioned examples highlight the application of our analytical stability criteria in constraining the possible configurations of hidden planets. In particular, GR precession induced by the star can increase the stabilization of a multi-planet system against perturbation from a far away companion. Further, we showed that GR precession could also stabilize an ultra-short period hidden planet, even in the presence of resonances induced by a multi-planet system.

[7] Note that such a planet will not survive Kepler-56 radial expansion as it continues to evolve (Li et al. 2014b), but it may result in some ejections from the star (e.g., Stephan et al. 2020).

ACKNOWLEDGEMENTS

We thank Matt Payne for his `Mercury` version with GR precession.We thank Gongjie Li for useful discussion and comments on an earlier version of the paper. Likewise, we would also like to thank Juliette Becker and Peter Plavchan, and Jon Zink. This research has made use of the NASA Exoplanet Archive, which is operated by the California Institute of Technology, under contract with the National Aeronautics and Space Administration under the Exoplanet Exploration Program. T.F and S.N. acknowledge partial support from the NSF through grant No. AST-1739160. S.N. thanks Howard and Astrid Preston for their generous support. L.W and S.N acknowledge the support from the Cross-Disciplinary Scholars in Science and Technology (CSST) program of University of California, Los Angeles.

REFERENCES

Antognini, J. M. O. 2015, MNRAS, 452, 3610, doi: 10.1093/mnras/stv1552

Ballard, S., & Johnson, J. A. 2016, ApJ, 816, 66, doi: 10.3847/0004-637X/816/2/66

Barbato, D., Sozzetti, A., Desidera, S., et al. 2018, A&A, 615, A175, doi: 10.1051/0004-6361/201832791

Barclay, T., Rowe, J. F., Lissauer, J. J., et al. 2013, Nature, 494, 452, doi: 10.1038/nature11914

Barros, S. C. C., Gosselin, H., Lillo-Box, J., et al. 2017, A&A, 608, A25, doi: 10.1051/0004-6361/201731276

Becker, J., Batygin, K., Fabrycky, D., et al. 2020, AJ, 160, 254, doi: 10.3847/1538-3881/abbad3

Bonomo, A. S., Desidera, S., Benatti, S., et al. 2017, A&A, 602, A107, doi: 10.1051/0004-6361/201629882

Borucki, W. J. 2016, Reports on Progress in Physics, 79, 036901, doi: 10.1088/0034-4885/79/3/036901

Boué, G., & Fabrycky, D. C. 2014, ApJ, 789, 111, doi: 10.1088/0004-637X/789/2/111

Bryan, M. L., Knutson, H. A., Lee, E. J., et al. 2019, AJ, 157, 52, doi: 10.3847/1538-3881/aaf57f

Bryan, M. L., Knutson, H. A., Howard, A. W., et al. 2016, ApJ, 821, 89, doi: 10.3847/0004-637X/821/2/89

Carrera, D., Ford, E. B., & Izidoro, A. 2019, MNRAS, 486, 3874, doi: 10.1093/mnras/stz974

Chambers, J. E. 1999, MNRAS, 304, 793, doi: 10.1046/j.1365-8711.1999.02379.x

Chatterjee, S., Ford, E. B., Matsumura, S., & Rasio, F. A. 2008, ApJ, 686, 580, doi: 10.1086/590227

Christiansen, J. L. 2017, Planet Detection Metrics: Pixel-Level Transit Injection Tests of Pipeline Detection Efficiency for Data Release 25, Kepler Science Document KSCI-19110-001

Christiansen, J. L., Jenkins, J. M., Caldwell, D. A., et al. 2012, PASP, 124, 1279, doi: 10.1086/668847

Crossfield, I. J. M., Ciardi, D. R., Isaacson, H., et al. 2017, AJ, 153, 255, doi: 10.3847/1538-3881/aa6e01

Dai, F., Winn, J. N., Gandolfi, D., et al. 2017, AJ, 154, 226, doi: 10.3847/1538-3881/aa9065

Denham, P., Naoz, S., Hoang, B.-M., Stephan, A. P., & Farr, W. M. 2019, MNRAS, 482, 4146, doi: 10.1093/mnras/sty2830

Dobbs-Dixon, I., Lin, D. N. C., & Mardling, R. A. 2004, ApJ, 610, 464, doi: 10.1086/421510

Fabrycky, D., & Tremaine, S. 2007, ApJ, 669, 1298, doi: 10.1086/521702

Fabrycky, D. C., Johnson, E. T., & Goodman, J. 2007, ApJ, 665, 754, doi: 10.1086/519075

Fang, J., & Margot, J.-L. 2012, ApJ, 761, 92, doi: 10.1088/0004-637X/761/2/92

Ford, E. B., Joshi, K. J., Rasio, F. A., & Zbarsky, B. 2000, ApJ, 528, 336, doi: 10.1086/308167

Frustagli, G., Poretti, E., Milbourne, T., et al. 2020, A&A, 633, A133, doi: 10.1051/0004-6361/201936689

Gandolfi, D., Fossati, L., Livingston, J. H., et al. 2019, ApJL, 876, L24, doi: 10.3847/2041-8213/ab17d9

Gilbert, G. J., & Fabrycky, D. C. 2020, AJ, 159, 281, doi: 10.3847/1538-3881/ab8e3c

Gupta, A., & Schlichting, H. E. 2020, MNRAS, 493, 792, doi: 10.1093/mnras/staa315
—. 2021, MNRAS, 504, 4634, doi: 10.1093/mnras/stab1128
Hadden, S., & Lithwick, Y. 2014, ApJ, 787, 80, doi: 10.1088/0004-637X/787/1/80
Hansen, B. M. S. 2009, ApJ, 703, 1131, doi: 10.1088/0004-637X/703/1/1131
Hansen, B. M. S. 2017, MNRAS, 467, 1531, doi: 10.1093/mnras/stx182
Hansen, B. M. S., & Murray, N. 2013, ApJ, 775, 53, doi: 10.1088/0004-637X/775/1/53
Hansen, B. M. S., & Naoz, S. 2020, MNRAS, 499, 1682, doi: 10.1093/mnras/staa2602
Hatzes, A. P., Guenther, E. W., Endl, M., et al. 2005, A&A, 437, 743, doi: 10.1051/0004-6361:20052850
He, M. Y., Ford, E. B., & Ragozzine, D. 2021, AJ, 162, 216, doi: 10.3847/1538-3881/ac1db8
Holman, M. J., & Wiegert, P. A. 1999, AJ, 117, 621, doi: 10.1086/300695
Howard, A. W., Marcy, G. W., Johnson, J. A., et al. 2010, Science, 330, 653, doi: 10.1126/science.1194854
Howard, A. W., Marcy, G. W., Bryson, S. T., et al. 2012, ApJS, 201, 15, doi: 10.1088/0067-0049/201/2/15
Huber, D., Carter, J. A., Barbieri, M., et al. 2013, Science, 342, 331, doi: 10.1126/science.1242066
Innanen, K. A., Zheng, J. Q., Mikkola, S., & Valtonen, M. J. 1997, AJ, 113, 1915, doi: 10.1086/118405
Knutson, H. A., Fulton, B. J., Montet, B. T., et al. 2014, ApJ, 785, 126, doi: 10.1088/0004-637X/785/2/126
Konopacky, Q. M., Rameau, J., Duchêne, G., et al. 2016, The Astrophysical Journal, 829, L4, doi: 10.3847/2041-8205/829/1/l4
Kozai, Y. 1962, AJ, 67, 591, doi: 10.1086/108790
Lai, D., Anderson, K. R., & Pu, B. 2018, MNRAS, 475, 5231, doi: 10.1093/mnras/sty133
Li, G., Dai, F., & Becker, J. 2020, ApJL, 890, L31, doi: 10.3847/2041-8213/ab72f4
Li, G., Naoz, S., Kocsis, B., & Loeb, A. 2014a, ApJ, 785, 116, doi: 10.1088/0004-637X/785/2/116
Li, G., Naoz, S., Valsecchi, F., Johnson, J. A., & Rasio, F. A. 2014b, ApJ, 794, 131, doi: 10.1088/0004-637X/794/2/131
Lidov, M. L. 1962, Planet. Space Sci., 9, 719, doi: 10.1016/0032-0633(62)90129-0
Lissauer, J. J., Ragozzine, D., Fabrycky, D. C., et al. 2011, ApJS, 197, 8, doi: 10.1088/0067-0049/197/1/8
Liu, B., Muñoz, D. J., & Lai, D. 2015, MNRAS, 447, 747, doi: 10.1093/mnras/stu2396
Livingston, J. H., Endl, M., Dai, F., et al. 2018, AJ, 156, 78, doi: 10.3847/1538-3881/aaccde
Loyd, R. O. P., Shkolnik, E. L., Schneider, A. C., et al. 2020, ApJ, 890, 23, doi: 10.3847/1538-4357/ab6605
Malavolta, L., Mayo, A. W., Louden, T., et al. 2018, AJ, 155, 107, doi: 10.3847/1538-3881/aaa5b5
Malhotra, R. 2015, ApJ, 808, 71, doi: 10.1088/0004-637X/808/1/71
Mardling, R. A., & Lin, D. N. C. 2004, ApJ, 614, 955, doi: 10.1086/423794
Martin, D. V., Mazeh, T., & Fabrycky, D. C. 2015, MNRAS, 453, 3554, doi: 10.1093/mnras/stv1870
Mayo, A. W., Vanderburg, A., Latham, D. W., et al. 2018, AJ, 155, 136, doi: 10.3847/1538-3881/aaadff
Ment, K., Fischer, D. A., Bakos, G., Howard, A. W., & Isaacson, H. 2018, AJ, 156, 213, doi: 10.3847/1538-3881/aae1f5
Michtchenko, T. A., & Malhotra, R. 2004, Icarus, 168, 237, doi: 10.1016/j.icarus.2003.12.010
Millholland, S. C., & Spalding, C. 2020, ApJ, 905, 71, doi: 10.3847/1538-4357/abc4e5
Mills, S. M., Howard, A. W., Weiss, L. M., et al. 2019, AJ, 157, 145, doi: 10.3847/1538-3881/ab0899
Moe, M., & Di Stefano, R. 2015, ApJ, 801, 113, doi: 10.1088/0004-637X/801/2/113
Morbidelli, A., & Crida, A. 2007, Icarus, 191, 158, doi: 10.1016/j.icarus.2007.04.001
Murchikova, L., & Tremaine, S. 2020, AJ, 160, 160, doi: 10.3847/1538-3881/abab9e
Murray, C. D., & Dermott, S. F. 2000, Solar System Dynamics, ed. Murray, C. D. & Dermott, S. F.
Naoz, S. 2016, ARA&A, 54, 441, doi: 10.1146/annurev-astro-081915-023315
Naoz, S., Farr, W. M., Lithwick, Y., Rasio, F. A., & Teyssandier, J. 2011, Nature, 473, 187, doi: 10.1038/nature10076
—. 2013a, MNRAS, 431, 2155, doi: 10.1093/mnras/stt302
Naoz, S., Farr, W. M., & Rasio, F. A. 2012, ApJL, 754, L36, doi: 10.1088/2041-8205/754/2/L36
Naoz, S., Kocsis, B., Loeb, A., & Yunes, N. 2013b, ApJ, 773, 187, doi: 10.1088/0004-637X/773/2/187
NASA Exoplanet Archive. 2022, Planetary Systems, Version: 2022-04-19 21:49, NExScI-Caltech/IPAC, doi: 10.26133/NEA12
Nesvold, E. R., Naoz, S., Vican, L., & Farr, W. M. 2016, ApJ, 826, 19, doi: 10.3847/0004-637X/826/1/19
Otor, O. J., Montet, B. T., Johnson, J. A., et al. 2016, AJ, 152, 165, doi: 10.3847/0004-6256/152/6/165
Owen, J. E., & Wu, Y. 2016, ApJ, 817, 107, doi: 10.3847/0004-637X/817/2/107
—. 2017, ApJ, 847, 29, doi: 10.3847/1538-4357/aa890a

Petigura, E. A. 2020, AJ, 160, 89, doi: 10.3847/1538-3881/ab9fff

Petrovich, C. 2015a, ApJ, 805, 75, doi: 10.1088/0004-637X/805/1/75

—. 2015b, ApJ, 799, 27, doi: 10.1088/0004-637X/799/1/27

Petrovich, C., Deibert, E., & Wu, Y. 2019, AJ, 157, 180, doi: 10.3847/1538-3881/ab0e0a

Plavchan, P., Chen, X., & Pohl, G. 2015, ApJ, 805, 174, doi: 10.1088/0004-637X/805/2/174

Pu, B., & Lai, D. 2018, MNRAS, 478, 197, doi: 10.1093/mnras/sty1098

—. 2019, MNRAS, 488, 3568, doi: 10.1093/mnras/stz1817

Pu, B., & Wu, Y. 2015, ApJ, 807, 44, doi: 10.1088/0004-637X/807/1/44

Raghavan, D., McAlister, H. A., Henry, T. J., et al. 2010, ApJS, 190, 1, doi: 10.1088/0067-0049/190/1/1

Raymond, S. N., & Izidoro, A. 2017, Icarus, 297, 134, doi: 10.1016/j.icarus.2017.06.030

Rice, K. 2015, MNRAS, 448, 1729, doi: 10.1093/mnras/stv073

Rodriguez, J. E., Zhou, G., Vanderburg, A., et al. 2017, AJ, 153, 256, doi: 10.3847/1538-3881/aa6dfb

Sanchis-Ojeda, R., Rappaport, S., Winn, J. N., et al. 2014, ApJ, 787, 47, doi: 10.1088/0004-637X/787/1/47

Schultz, K., Spalding, C., & Batygin, K. 2021, MNRAS, 506, 2999, doi: 10.1093/mnras/stab1899

Steffen, J. H., & Hwang, J. A. 2015, MNRAS, 448, 1956, doi: 10.1093/mnras/stv104

Stephan, A. P., Naoz, S., & Gaudi, B. S. 2018, AJ, 156, 128, doi: 10.3847/1538-3881/aad6e5

Stephan, A. P., Naoz, S., Gaudi, B. S., & Salas, J. M. 2020, ApJ, 889, 45, doi: 10.3847/1538-4357/ab5b00

Stock, S., Reffert, S., & Quirrenbach, A. 2018, A&A, 616, A33, doi: 10.1051/0004-6361/201833111

Takeda, G., Kita, R., & Rasio, F. A. 2008, ApJ, 683, 1063, doi: 10.1086/589852

Takeda, G., & Rasio, F. A. 2005, ApJ, 627, 1001, doi: 10.1086/430467

Tamayo, D., Cranmer, M., Hadden, S., et al. 2020, Proceedings of the National Academy of Science, 117, 18194, doi: 10.1073/pnas.2001258117

Teyssandier, J., Naoz, S., Lizarraga, I., & Rasio, F. A. 2013, ApJ, 779, 166, doi: 10.1088/0004-637X/779/2/166

Touma, J. R., Tremaine, S., & Kazandjian, M. V. 2009, MNRAS, 394, 1085, doi: 10.1111/j.1365-2966.2009.14409.x

Veras, D., & Ford, E. B. 2010, ApJ, 715, 803, doi: 10.1088/0004-637X/715/2/803

Walsh, K. J., Morbidelli, A., Raymond, S. N., O'Brien, D. P., & Mandell, A. M. 2011, Nature, 475, 206, doi: 10.1038/nature10201

Wei, L., Naoz, S., Faridani, T., & Farr, W. M. 2021, ApJ, 923, 118, doi: 10.3847/1538-4357/ac2c70

Weiss, L. M., & Petigura, E. A. 2020, The Astrophysical Journal, 893, L1, doi: 10.3847/2041-8213/ab7c69

Weiss, L. M., Marcy, G. W., Petigura, E. A., et al. 2018a, AJ, 155, 48, doi: 10.3847/1538-3881/aa9ff6

Weiss, L. M., Isaacson, H. T., Marcy, G. W., et al. 2018b, AJ, 156, 254, doi: 10.3847/1538-3881/aae70a

Wu, Y., Murray, N. W., & Ramsahai, J. M. 2007, ApJ, 670, 820, doi: 10.1086/521996

Xie, J.-W., Dong, S., Zhu, Z., et al. 2016, Proceedings of the National Academy of Science, 113, 11431, doi: 10.1073/pnas.1604692113

Xiu-Min, H., & Jiang-Hui, J. 2020, ChA&A, 44, 283, doi: 10.1016/j.chinastron.2020.08.001

Zhou, G., Rodriguez, J. E., Vanderburg, A., et al. 2018, AJ, 156, 93, doi: 10.3847/1538-3881/aad085

Zhu, W. 2020, AJ, 159, 188, doi: 10.3847/1538-3881/ab7814

Zhu, W., & Wu, Y. 2018, AJ, 156, 92, doi: 10.3847/1538-3881/aad22a